Application of the Transient Dual Interface Method in Test Based Modeling of Heat-sinks Aimed at Socketable LED Modules

András Poppe[1,2], Gusztáv Hantos[1], János Hegedűs[1]
[1]Budapest University of Technology, Department of Electron Devices
Magyar tudósok körútja 2, bldg Q, H-1117
Budapest/Hungary
poppe@eet.bme.hu

[2]Mentor Graphics Mechanical Analysis Division
Gábor Dénes utca 2, H-1117
Budapest/Hungary
andras_poppe@mentor.com

Abstract

This paper presents a method of thermal characterization of heat-sinks aimed at cooling socketable LED modules. The suggested measurement procedure resembles the transient dual interface method of the JEDEC JESD51-14 standard: two transient measurements are performed with different qualities of the thermal interface of the heat-sink surface mating the LED modules. The structure functions section identified with such a measurement represents solely the measured heat-sink. Step wise approximation of the obtained structure function section is used to create DCTMs of the heat-sinks, aimed at fast system level simulations of LED modules.

Keywords

socketable LED module, heat-sink compact modeling, test based modeling

1. Introduction

The concept of compact thermal modeling of semiconductor device packages as well as heat-sinks based on thermal transient measurements of power transistors and CPUs, using structure functions was introduced about a decade ago [1]. Though the method outlined in this early paper provided quantified results to describe heat-sinks, no standardized method was provided to separate the device package, the TIM and the heat-sink in the structure functions. A recent report discussed the design optimization of heat-sinks aimed at cooling of CoB LED arrays [2], but the results presented in this paper are based mostly on simulation and are characteristic to the entire LED array + heat-sink assembly; do not provide quantified characteristics for the heat-sinks separately.

The so called transient dual interface method (TDM) defined in the JEDEC JESD 51-14 standard [3] provides well repeatable means of separating sections of the junction-to-ambient heat-removal path of packaged semiconductor devices. The standard is aimed at the measurement of the R_{thJC} junction-to-case thermal resistance of power semiconductor packages. This method, e.g. with the help of structure functions is used to find the initial part of the heat-conduction path: from the junction until a "virtual boundary" of the package characterized by the single R_{thJC} value. The "rest" of the structure functions used in the method is disregarded. Essential part of the JESD 51-14 test method is to perform the thermal transient measurements of the DUT on a cold-plate, therefore the discarded part of the structure functions – in terms of the corresponding cumulative thermal resistance – is short; it is characteristic mostly to the thermal interface between the package and the cold-plate as illustrated in Figure 1.

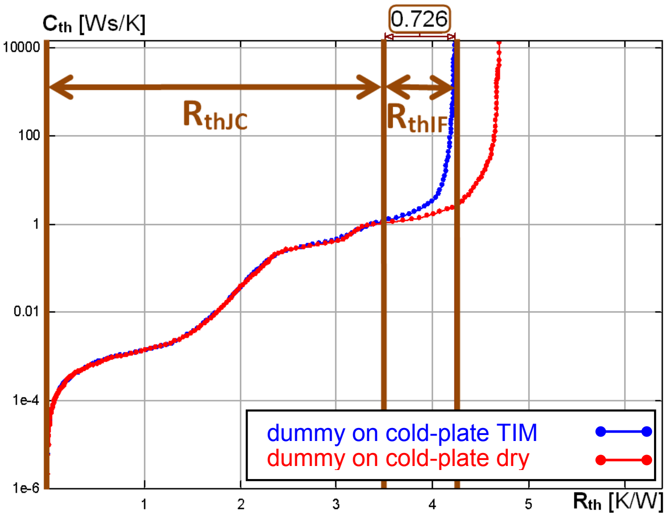

Figure 1: Structure functions of a test module measured on a cold-plate with and without applying TIM at the module – cold-plate interface. The separation point of the two curves is defined as R_{thJC}.

2. Measurements

To characterize heat-sinks aimed at the cooling of socketable LED modules such as GE's Infusion family [4], we built a thermal dummy module which mimics the behavior of the LED modules at the module – heat-sink mechanical interface properly [5]. All the examples presented here are based on test results obtained with this test module. The heat-sinks we characterized are shown in Figure 2.

The benefit of using a thermal dummy of the socketable LED module was that we could avoid the difficulty arising from the need of measuring the module + heat-sink assemblies under natural convection conditions while existing LED thermal testing standards (JESD 51-5x series) require light output measurements of LEDs at a controlled temperature. As in the thermal dummy of the LED module a conventional silicon device was used, we could adhere to the simpler thermal testing standard (JESD 51-1), see further details in [5]. As described in [5] the thermal dummy module was constructed such that the heat-flow pattern close to the modules cooling surface (the so called thermal interface according to the Zhaga terminology [6]) the heat-flow pattern is the same as in the original LED module.

As shown in Figure 1, the test module was characterized on a cold-plate with a procedure based on the JEDEC JESD51-14 standard [3]. This way we identified a junction-to-case thermal resistance value (denoted by R_{thJC} in Figure 1) which we considered as an overall characteristic of the module representing the steady-state behavior of the heat-flow path of the module between the pn-junction of the module's active device and the bottom surface of the module which under normal operating conditions mates with the central circular surface of the heat-sink (see Figure 2a). The thermal transient measurements of the heat-sinks were carried out in a natural convection environment resembling a JEDEC standard 1 ft^3 still-air chamber. The test module was attached to the heat-sinks with the help of a LED module socket assembled to the heat-sink (as shown in Figure 2b). The clamping force between the test module and the heat-sink was provided by the springs inside the socket.

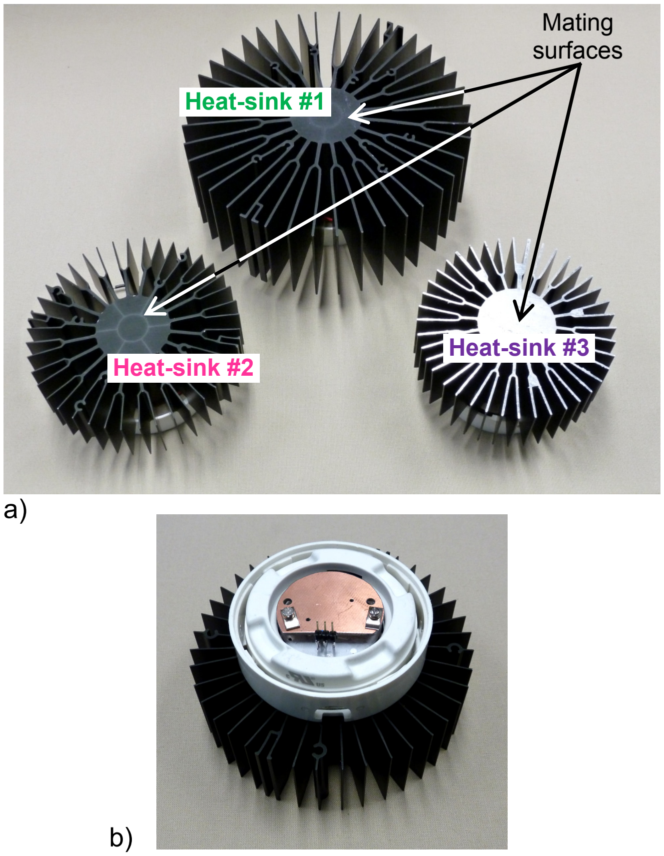

Figure 2: a) Three different heat-sinks which were characterized by a thermal dummy of a socketable LED module b) The thermal dummy module in the socket attached to heat-sink #1.

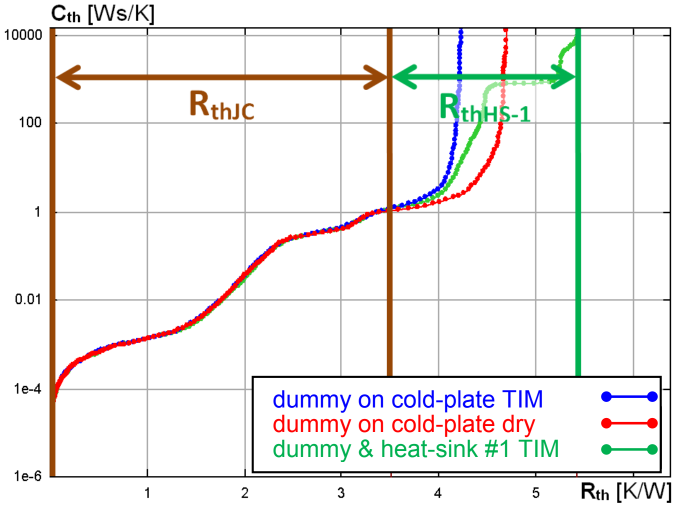

Figure 3: Comparison of structure functions of Figure 1 and a structure function identified when the test module was equipped with heat-sink #1.

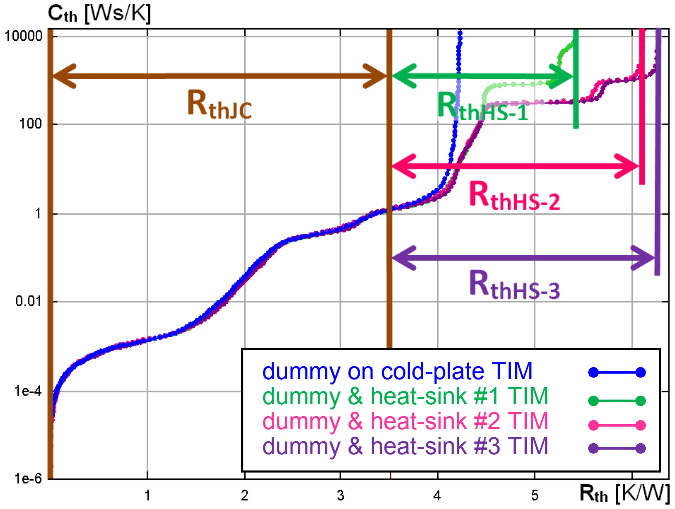

Figure 4: Comparison of structure functions of three different heat-sinks measured in a natural convection environment and the base line test setup of the dummy module measured on cold-plate.

Under normal operating conditions the bottom of the socketable LED modules (their thermal interface) is covered by a thermal pad – an elastic thermal interface material. During our tests the thermal pad was removed and no TIM was applied or ordinary thermal grease was used as TIM to realize a second boundary condition recommended by the JEDEC JESD51-14 standard [3].

With further measurements where the quality of the thermal interface between the heat-sink and the test module (in our case a thermal dummy of a LED module) is changed and the resulting structure functions are matched at their ends (at the singularity) the contribution of the TIM and the contribution of the heat-sink to the total thermal resistance is separated.

2.1. Measurement results

The thermal resistance values indicated as R_{thIF} in Figure 1 provides the interfacial thermal resistance at the module's cooling surface.

The thermal boundary conditions provided by the three different heat-sinks clamped to the test module with thermal grease as TIM provide worse cooling than TIM cold-plate + TIM setup but provide still better cooling compared to the case when the test module was attached to a cold-plate without any TIM (referred to as "cold-plate dry" setup in all Figures). To demonstrate this, in Figure 3 a third structure function is included along with the cold-plate measurement results. This structure function was identified when the test module was equipped with a heat-sink and was measured in a natural convection environment. All structure function sections representing the heat-flow still inside the test module completely overlap. The green structure function section seen in Figure 3 characterizes the applied heat-sink. In Figure 4 results for further two heat-sinks are shown.

As expected, the largest heat-sink (heat-sink #1) provides the smallest thermal resistance but it has the largest thermal capacitance (see the height of the flat green section) – see seen Figure 4. Heat-sinks #2 and #3 provide almost the same cooling performance with the same thermal capacitances and only with a small difference (roughly 0.1 K/W) in the overall thermal resistance. Resistances denoted by R_{thHS-1}, R_{thHS-2} and R_{thHS-3} in Figure 4provide additional the thermal resistance of the module – heat-sink thermal interface and the heat-sink. All these measurement results were obtained for a setup when TIM was applied between the mating surfaces of the test module and the heat-sinks.

Figure 5 presents results of the measurements of heat-sink #2 when the heat-sink was measured without applying TIM at the interface mating with the test module.

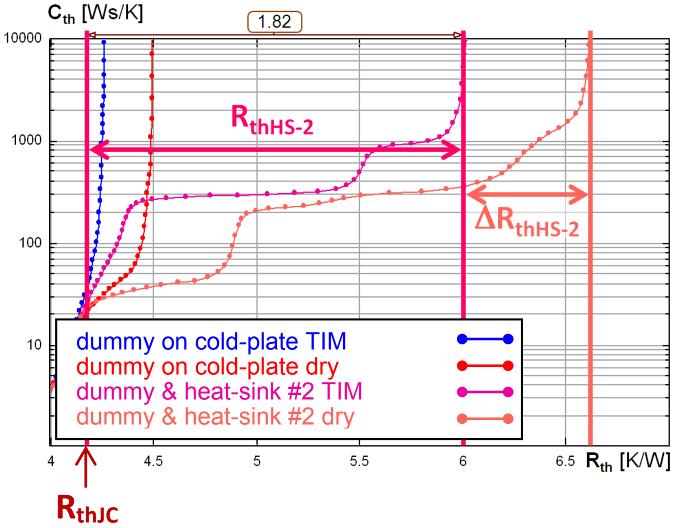

Figure 5: Close-up view of the structure functions already shown in Figures 1, 2 and 3 with thermal resistance of heat-sink #2 indicated. The plot of the structure function representing the thermal impedance when no TIM was applied between the test module and the heat-sink is also included.

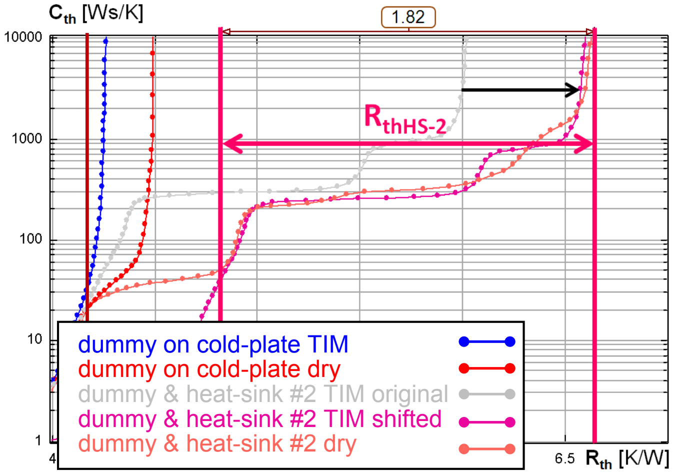

Figure 6: Modified version of Figure 5 – the structure function representing the heat-sink + TIM setup is matched at the ambient with the structure function of the heat-sink + no TIM setup. The divergence point of these curves on the left corresponds to the mating surface of the heat-sink.

In Figure 5 the numerical value of the R_{thHS-2} thermal resistance is also indicated (1.82 K/W) Note in Figure 5 that the structure function of the "dry" setup also starts diverging from the other structure functions at the "case" location (indicated by R_{thJC} in the figure) but now providing worse cooling than the "dry" interface at the cold-plate setup. As expected, due to the poor quality of the thermal interface at the heat-sink the overall thermal resistance is increased. This excess resistance is denoted by ΔR_{thHS-2} in the figure and its value is roughly 1.13 K/W.

2.2. Application of the transient dual interface principle to the characterization of heat-sinks

In Figure 7 the original structure function of the test module + TIM + heat-sink setup was shifter to the right to match the structure function of the "dry" setup at the singularity corresponding to the ambient. The structure functions measured with the heat-sink almost perfectly at the initial sections corresponding to heat-spreading still within the body of the heat sink; the difference on the left hand side of the middle thick vertical indicator line are due to the drastic differences in the quality of the thermal interface between the heat-sink and the test module (TIM applied vs. "dry" interface). The distance of this divergence point from the ambient is equal to the R_{thHS-2} value. We had similar findings for the other two heat-sinks as well.

Form this result we can conclude that the philosophy of the transient dual interface method for the measurement of the junction-to-case thermal resistance of the power semiconductor device packages with a single heat-flow path between their junction and their exposed cooling surface can also be applied for the characterization of heat-sinks as well. A plausible condition for this is that the heat-flow entering the heat-sink at the mating surface with the device to be cooled should still be an essentially one-dimensional one. (Further away from the mating surface inside the body of a heat-sink when more complex heat-spreading patterns exist and at the fin-air interfaces were natural convection starts, the structure functions provide only an equivalent model of the thermal impedance. This corresponds only to the last, very small section of the structure function.)

This means that it is sufficient to carry out thermal transient measurements of the test module with a heat-sink attached in a natural convection test environment twice: once with a poor quality of the thermal interface ("dry" mating surface, i.e. no TIM applied) and once with a good quality of the thermal interface (TIM applied). The difficulty is to provide identical test conditions for both measurements. Then the measured thermal impedances have to be converted into (cumulative) structure functions and their need to be matched at the ambient side (at the singularity at the right hand side) and the divergence point between the two curves need to be identified. The structure function section between this divergence point and the singularity is characteristic to the heat-sink; the distance between this divergence point and the singularity is equal to the overall thermal resistance (denoted by $R_{thHS\text{-}2}$ in Figure 6) of the heat-sink. This value of course depends on the test conditions, for example it is influenced by the orientation of the heat-sink (normal position, upside-down or tilted – as it may vary especially in case of LED modules when used in different luminaires).

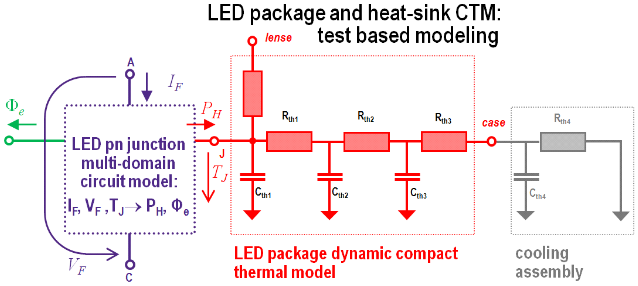

Figure 7: LED pn-junction multi-domain model completed with test based package and heat-sink compact thermal model [8], [9].

3. Dynamic compact modeling of heat-sinks

The step-wise approximation of the structure functions first suggested to model MCPCB based LED assemblies [7] can also be applied to the structure function sections representing heat-sinks. This way more advanced and more accurate heat-sink compact models can be created than first suggested in [1]. Though structure functions are primarily aimed to represent essentially 1D heat-conduction cases they can also be used as black-box equivalent models for complex 3D heat-transfer like heat-sinks.

As suggested in [8] and [9] dynamic compact thermal models of cooling assemblies such as heat-sinks can be attached to the multi-domain models of LED pn-junctions completed by compact thermal models of the LED packages, aimed at Spice-like simulation. This also applies to socketable LED modules: the LED package compact thermal model can be extended with RC stages representing additional structural elements of an LED module (MCPCB, module heat-slug, etc.). Figure 7 illustrates this application of heat-sink models, though, as seen both in Figure 4 and in Figure 5, a single RC stage would not be appropriate for the actual heat-sinks presented here.

Compared to first attempt to structure function based compact modeling of heat-sinks briefly described in an early paper of our team [1] the "transient dual interface method" like test procedure presented in section 2.2 provides now a well-defined method of locating the "beginning" of the heat-sinks along the heat-flow path.

The method already provided a single thermal resistance value (see $R_{thHS\text{-}2}$ in Figure 5 and in Figure 6) which can be used for steady-state simulations.

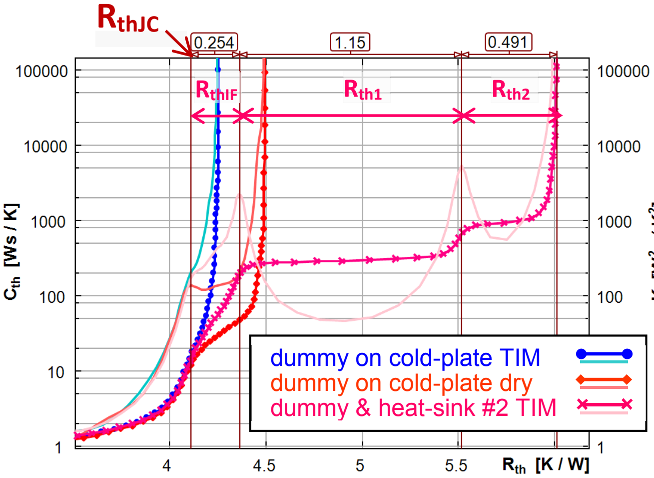

Figure 8: Partial thermal resistances of the thermal interface and the heat-sink can be identified with the help of the differential structure functions (plotted with thinner lines using lighter colors).

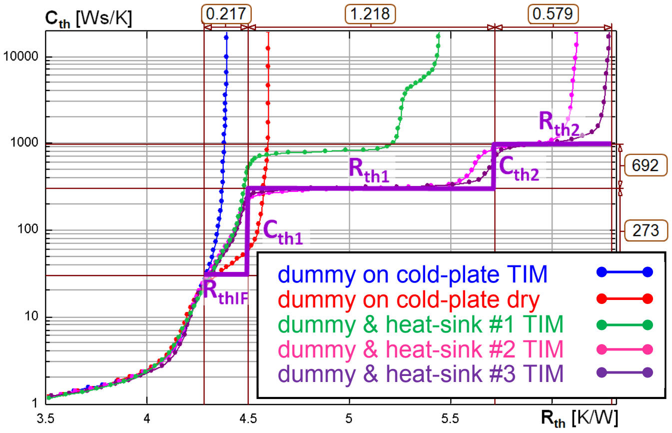

Figure 9: Step-wise approximation of the cumulative structure function at the section corresponding to the heat-sink results in a dynamic thermal compact model of the heat-sink. The interface thermal resistance between the LED module and the heat-sink denoted by R_{thIF} is also identified.

In case of LED modules and complete luminaires however, a major parameter of interest for lighting designers is the time needed to reach the final, stable value of the luminous flux which is the time to reach thermal steady-state of the LED's pn-junction. To calculate this time by simulation needs a dynamic thermal model of both the LED package or LED module and the applied heat-sink.

3.1. Step-wise approximation of the cumulative structure function

As seen in the structure function sections representing the heat-sinks we measured, there are multiple steps. This suggests that there are multiple characteristic parts of the heat-sinks. The first step in creating a multiple stage RC model of the heat-sinks is to identify the partial thermal resistances: the peaks of the differential structure functions help in this. These peaks represent steep transitions in the cumulative structure functions.

In Figure 8 we plotted both the cumulative structure functions and the differential structure functions corresponding to the two base-line setups (test module measured on a cold-plate with and without applying TIM) and corresponding to the setup when the test module was attached to the heat-sink #2 with the application of thermal grease at the mating surfaces.

Starting with the location denoted by R_{thJC} in Figure 8, before the singularity representing the ambient we have 3 peaks in the differential structure function of heat-sink #2 (plotted with a thin, light pink line in the presented diagram), thus we can distinguish 3 different sections. The first one is the thermal interface, its resistance is denoted by R_{thIF}. The further two sections correspond to the heat-spreading in the central part of the heat-sink (described by the thermal resistance value R_{th1}) and the heat-spreading in the fins and the heat-transfer from the fins to the surrounding air (represented by the equivalent thermal resistance R_{th2})

The next step is to identify the thermal capacitance values corresponding to the above parts of the heat-sink. These correspond to the heights of the flat sections of the cumulative structure functions (plotted by a thick, pink line in Figure 8). The best matching approximation can be found by a straight horizontal line crossing the cumulative structure function at the inflection points of these flat sections. These points can be found at the minima of the differential structure functions. The distances between these straight horizontal lines provide the required thermal capacitance values for the compact model (see C_{th1} and C_{th2} in Figure 9).

Based on this approximation method element values of the RC compact model of heat-sink #3 are shown in Figure 9. The differences between the thermal resistance values of heat-sink #2 and #3 are explained by the difference in the quality of the mating surfaces and the slight geometry differences of the two heat-sinks (see also Figure 2a).

This step-wise approximation of the structure function representing the heat-sinks is the generalization of the test based compact modeling method first suggested for the test based compact thermal modeling power LED packages [7].

3.2. Application example

System level simulation using LED compact models is among the possible applications of the dynamic compact thermal models of the heat-sinks. In the example below the compact model of a real socketable LED module was created from measurements. The R_{thJC} junction-to-case thermal resistance of the module was 1.75 K/W (without the thermal pad attached to the module). This value was identified with the transient dual interface method of the JESD51-14 standard based in two measurements compliant with the JESD51-51 and JESD51-52 LED thermal testing standards. The measured structure functions and the identified LED module dynamic thermal compact model (DCTM) are shown in Figure 10.

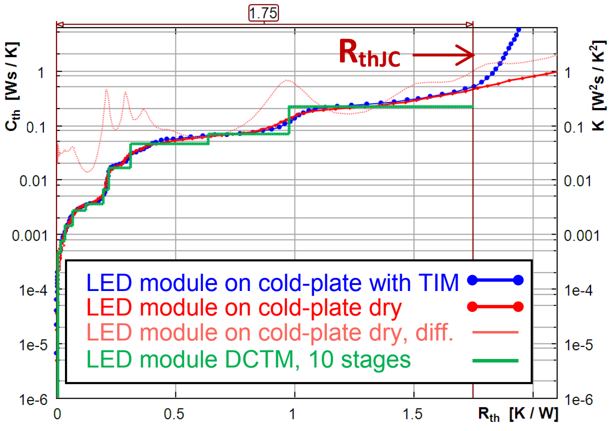

```
@SUBCIRCUIT LED_MODULE(CASE)=POWER;
   C0: THCAP(J,GND)=1.360840e-004;
   R0: THRES(J,N1)=9.602051e-003;
   C1: THCAP(N1,GND)=5.120376e-004;
   R1: THRES(N1,N2)=2.251920e-002;
   C2: THCAP(N2,GND)=9.342327e-004;
   R2: THRES(N2,N3)=3.348633e-002;
   C3: THCAP(N3,GND)=1.488764e-003;
   R3: THRES(N3,N4)=5.324765e-002;
   C4: THCAP(N4,GND)=1.011053e-003;
   R4: THRES(N4,N5)=7.358012e-002;
   C5: THCAP(N5,GND)=3.340653e-003;
   R5: THRES(N5,N6)=2.099345e-002;
   C6: THCAP(N6,GND)=1.131491e-002;
   R6: THRES(N6,N7)=9.502891e-002;
   C7: THCAP(N7,GND)=3.297544e-002;
   R7: THRES(N7,N8)=3.234656e-001;
   C8: THCAP(N8,GND)=2.452578e-002;
   R8: THRES(N8,N9)=3.404372e-001;
   C9: THCAP(N9,GND)=1.654788e-001;
   R9: THRES(N9,CASE)=7.776395e-001;
   S1: HEATFLUX(GND,J)=POWER;
@END;
```

Figure 10: Measured structure functions (cumulative and differential) and the 10 stage thermal RC ladder model (DCTM) of a socketable LED module.

For the simulation the THERMAN program was used which is aimed at fast thermal simulation of homogeneous laminated structures and is extended with the capability of using DCTMs of semiconductor device packages and heat-sinks [10]. In the simulation example a material layer representing the module's thermal pad was used a "substrate". The DCTM of the heat-sink was attached to it at the top while the DCTM of the LED module was attached to it at the bottom, describing the thermal behavior of the LED module + heat-sink assembly used as a down-light luminaire. The DCTMs were executed by the built-in network solver of THERMAN

The heat-sink DCTM is a boundary condition dependent model. The netlist of such a model created for down-light applications is provided in Figure 11; the element values were obtained from the structure function shown in Figure 8. Figure 12 presents the junction temperature transient measured with the module attached to a cold-plate and the simulated transient of the module using the DCTM of heat-sink #2 assuming a physical arrangement of a down-light application. According to the simulation the time needed for reaching thermal steady-state is about 6200 s.

```
@SUBCIRCUIT HS2(CONTACT);
   RTHIF: THRES(CONTACT,N1)=0.254;
   CTH1: THCAP(N1,GND)=273;
   RTH1: THRES(N1,N2)=1.15;
   CTH2: THCAP(N2,GND)=692;
   RTH1: THRES(N2,GND)=0.491;
@END;
```

Figure 11: The netlist of the dynamic compact thermal model of heat-sink #2 in the format used by the THERMAN program [10].

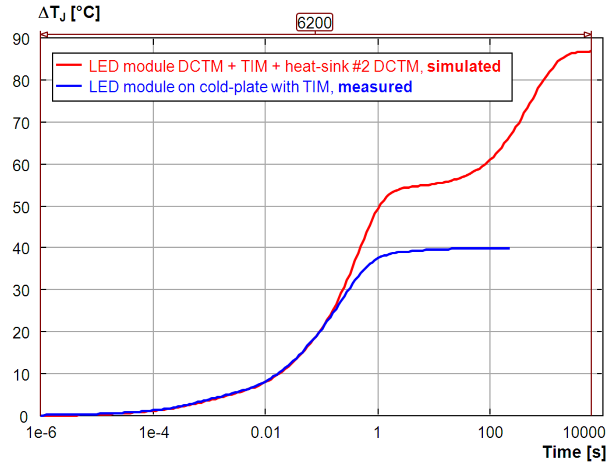

Figure 12: Comparison of the step response of the LED module measured on a cold-plate and simulated with the heat-sink model. In the simulation the measured actual LED heating power was used.

4. Conclusions

In this paper we presented a method to characterize heat-sinks aimed at the cooling of socketable LED modules. The actual thermal transient measurements of the heat-sinks took place in a natural convection environment using a thermal dummy module representing the original LED modules. In this test module a conventional silicon device was used as an active device. We applied the transient dual interface principle to identify location of the heat-sinks in the measured structure functions. The step-wise approximation of the structure function section representing the heat-sinks was used to create a multi-stage RC ladder model as a DCTM of heat-sinks aimed at system level simulations. Simulation of a free hanging down-light application was used to demonstrate the application of such heat-sink models.

Acknowledgments

The support of GE Lighting Hungary by providing test samples is acknowledged. We also thank Ernő Kollár for performing the first measurements and building the thermal dummy of GE's LED modules used in this work as a test module.

References

1. Gábor Farkas, András Poppe, Ernő Kollár, Peter Stehouwer, "Dynamic Compact Models of Cooling Mounts for Fast Board Level Design", In: Proceedings of the 19th IEEE Semiconductor Thermal Measurement and Management Symposium (SEMI-THERM'03), San Jose, USA, 11-13 March 2003, pp. 255-262,
2. Bum-Sik Seo, Ki-Joung Lee, Jong-Kyung Yang, Young Seek Cho, and Dae-Hee Park, "Development and Characterization of Optimum Heat Sink for 30 W Chip on Board LED Down-Light", TRANSACTIONS ON ELECTRICAL AND ELECTRONIC MATERIALS 13(6): pp. 292-296, 2012,
3. JEDEC JESD51-14 Standard "Tranisent Dual Interface Test Method for the Measurement of the Thermal Resistance Junction-To-Case of Semiconductor Devices with Heat Flow Through a Single Path", http://www.jedec.org/sites/default/files/docs/JESD51-14_1.pdf
4. www.gelighting.com/LightingWeb/na/solutions/highlights/infusion-led-module/overview/
5. András Poppe, Ernő Kollár, Zoltán Tóth, János Simonovics, "Characterization of heat-sinks of socketable LED modules using thermal transient testing", In Proceedings of the 20th International Workshop on THERMal INvestigation of ICs and Systems (THERMINIC'14), 24-26 September 2014, Greenwich, UK, paper 3_2_1033
6. Zhaga Interface Specification Book 1: Overview and Common Information, www.zhagastandard.org/specifications/book-1.htm
7. A. Poppe, G. Farkas, V. Székely, Gy. Horváth, M. Rencz, "Multi-domain simulation and measurement of power LED-s and power LED assemblies", In: Proceedings of the 22nd IEEE Semiconductor Thermal Measurement and Management Symposium (SEMI-THERM'06). Dallas, USA, March 14-16 2006, pp. 191-198.
8. A. Poppe, "A step forward in multi-domain modeling of power LEDs", In: Proceedings of the 28th IEEE Semiconductor Thermal Measurement and Management Symposium (SEMI-THERM'12), 18-22 March 2012, San Jose, USA, pp. 325-330
9. A. Poppe, T. Temesvölgyi, "A General Multi-domain LED Model and its Validation by Means of AC Thermal Impedance", In: Proceedings of the 29th IEEE Semiconductor Thermal Measurement and Management Symposium (SEMI-THERM'13), 17-21 March 2013, San Jose, USA, pp. 137-142.
10. M. Rencz, V. Székely, A. Poppe, B. Courtois, "Inclusion of RC Compact Models of Packages into Board Level Thermal Simulation Tools", In: Proceedings of the 18th IEEE Semiconductor Thermal Measurement and Management Symposium (SEMI-THERM'02), 11-14 March 2002, San Jose, USA, pp. 71-76